Compensating Chromatic Dispersion and Phase Noise using Parallel AFB-MBPS For FBMC-OQAM Optical Communication System

Original Scientific Paper

Ahmed H. Abbas
Communication Engineering Department,
University of Technology- Iraq
coe.21.01@grad.uotechnology.edu.iq

Thamer M. Jamel
Communication Engineering Department,
University of Technology- Iraq
thamer.m.jamel@uotechnology.edu.iq

Abstract *– Filter Bank Multi-Carrier Offset-QAM (FBMC-OQAM) is one of the hottest topics in research for 5G multi-carrier methods because of its high efficiency in the spectrum, minimal leakage in the side lobes, zero cyclic prefix (CP), and multiphase filter design. Large-scale subcarrier configurations in optical fiber networks need the use of FBMC-OQAM. Chromatic dispersion is critical in optical fiber transmission because it causes different spectral waves (color beams) to travel at different rates. Laser phase noise, which arises when the phase of the laser output drifts with time, is a major barrier that lowers throughput in fiber-optic communication systems. This deterioration may be closely related among channels that share lasers in multichannel fiber-optic systems using methods like wavelength-division multiplexing with frequency combs or space-division multiplexing. In this research, we use parallel Analysis Filter Bank (AFB) equalizers in the receiver part of the FBMC OQAM Optical Communication system to compensate for chromatic dispersion (CD) and phase noise (PN). Following the equalization of CD compensation, the phase of the carriers in the received signal is tracked and compensated using Modified Blind Phase Search (MBPS). The CD and PN compensation techniques are simulated and analyzed numerically and graphically to determine their efficacy. To evaluate the FBMC's efficiency across various equalizers, 16-OQAM is taken into account. Bit Error Rate (BER), Optical Signal-to-Noise Ratio (OSNR), Q-Factor, and Mean Square Error (MSE) were the primary metrics we utilized to evaluate performance. Single-tap equalizer, multi-tap equalizer (N=3), ISDF equalizer with suggested Parallel Analysis Filter Banks (AFBs) (K=3), and MBPS were all set aside for comparison. When compared to other forms of Nonlinear compensation (NLC), the CD and PN tolerance attained by Parallel AFB equalization with MBPS is the greatest.*

Keywords*: Keywords- FBMC, OQAM, Optical fiber communication, chromatic dispersion (CD) compensation, multi carrier modulation, Phase Noise, Nonlinear Effects, Nonlinear Compensation (NLC)*

1. INTRODUCTION

For coherent fiber optical communication (FOC), FBMC-OQAM has emerged as the multi-carrier modulation (MCM) of choice because to its enormous spectral efficiency [1]. Out-of-band leakage is significantly reduced in FBMC-OQAM [2], making it more adaptive in its adjustment of wave dispersion. Reduced guard band interval and zero CP in FBMC improve the system's spectral efficiency even more than in traditional OFDM [3]. The cladding and core of a fiber optic transmission system often have a differing refractive index, which may impede or speed up communication depending on the wavelength of light being sent. This is because the colors of light behave differently as they travel through a fiber optic [4]. Using number of subcarriers in the FBMC OQAM transmission is the only solution to tolerate the CD flatten the channel coefficients up to the level of subcarriers. But increasing the subcarrier to transmit for a desired bandwidth increases the duration of symbol which induce the phase noise of fiber channel [5].

The spectrum of the laser's emitted light must be a delta function. However, phase shifts in the laser's output optical field make this impossible [6]. Due to the oscillations' origin in the laser's own spontaneous emission, a statistical correlation is impossible to establish. They provide a time-varying disturbance in the carrier phase, known as phase noise (PN). The chromatic dis-

persion (CD) and phase noise (PN) may be minimized at the shortest possible transmission distance by using a single-tap equalization technique. When the number of subcarriers in long-distance communications became large enough, it began to have an effect on the equalization used to tolerate CD. Therefore, even for long-haul communication, an improved and effective equalization approach is required to carry out the CD compensation [7]. Furthermore, the optimum spectrum efficiency in optical communication depends on multi tap and time domain-based equalizations. For optical systems based on FBMC-OQAM, this is a major area of attention for researchers. In this study, we provide a design for a parallel AFB and MBPS equalization for FBMC-OQAM optics, which may be used to compensate for CD and PN. Simulation of each approach with various settings is also used to study and evaluate the FBMC OQAM's efficiency. In order to verify the equalizers in an optical system, a sampling rate of 30 GHz is taken into account.

The forthcoming section of the paper is structured as follows: Review of literature is presented in section II for multiple equalizers which we taken for the analysis of CD and PN compensation in FBMC-OQAM. In section III FBMC OQAM in optical system model and section IV for proposed equalizer design as mathematical model. In section V we concentrate on the performance analysis. Conclusion of this paper is discussed in section VI.

2. CD AND PN COMPENSATION EQUALIZER TECHNIQUES

i. Iterative Soft Decision Feedback Equalization

Inter symbol interference (ISI) caused by CD may be mitigated using a single tap equalizer. Although some inter-carrier-interference (ICI) and inter-symbol interference (ISI) residuals are present in the received data. Iterative Soft Decision Feedback Equalizer (ISDFE) was presented to further enhance the system by [10]. The N-Tap frequency sampling equalization is used in this technique. Nonlinear phase noise in the optical FBMC-OQAM system's back propagation was also adjusted by ISDFE, as shown in Fig. 1.

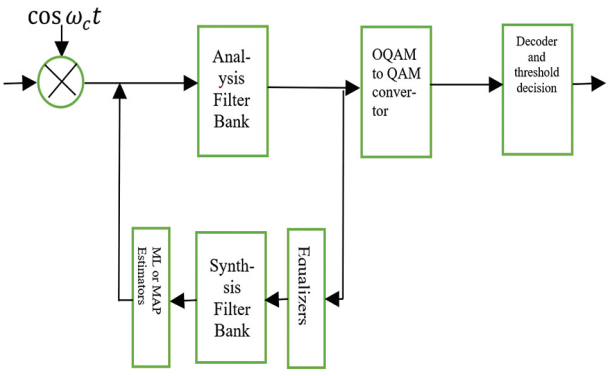

Fig. 1. ISDF equalizer

In the frequency domain, CD is a phase distortion, but in the time domain, NLP is a phase distortion.

The CD compensator (CDC) is used in the frequency domain to offset the effects of CD and NLP in the receiver.

$$H_{CD}(\omega) = \mathrm{e}^{-\left(\frac{jD}{2}\omega^2 L\right)+\delta} \tag{1}$$

where, D is second order dispersion known as group velocity dispersion (GVD) of fiber chromatic dispersion, L is fiber length, δ is phase shift and ω is angular frequency.

Repeatedly equalizing the CD by applying soft decision symbols (CDC output) and returning them to the SFB is how standard optical FBMC/OQAM achieves equalization of the CD. This is seen in Fig. 5. All leftover ISI is removed by passing to AFB several times during the operation, allowing the original signal to be reconstructed.

ii. Fourth-Order Nonlinearity

To eliminate the phase modulation in QPSK, the carrier phase may be approximated using a fourth-order nonlinearity, providing the estimate of the phase as follows:

$$\delta_{est}(n) = \left\{\frac{1}{2L+1}\sum_{q=-L}^{L} P(q)x_i^4(q+n)\right\} \tag{2}$$

where $P(q)$ is a weighting function that changes depending on how much laser phase noise is added to the additive white Gaussian noise [11]. For $P(q)$=1, Viterbi and Viterbi's estimator [12] is used as the estimator. A Wiener filter is used as a consequence of the weighting function to estimate the phase noise [13], which may perform almost as well as an ideal MAP estimator of the phase.

iii. Barycenter Algorithm

One particularly hardware-efficient phase estimator is the Barycenter algorithm [14] in which the order of the operations in Eq. (2) are reversed to give,

$$\delta_{est}(n) = \frac{1}{2L+1}\sum_{q=-L}^{L} P(q)\{x_i^4(q+n)\} \tag{3}$$

iv. Binary Phase Search (BPS)

Instead, the feedforward and parallelizable binary phase search (BPS) method may be utilized. The carrier phase is scanned from (0 to π/2 for square QAM), with the Euclidean distance between the rotating symbol and the final symbol being used to determine the mean square error for each trial phase. The iteration of the trial that yields the lowest MSE is chosen as the estimation iteration. In order to account for the ASE noise effect, the MSE is calculated by adding the distances between 2L symbols rotated by the same angle. As the decoding has already been completed during the testing step, the minimal mean squared error (MSE) index may be used to pick the decoded symbol through a toggle. Despite BPS's impressive tolerance for laser phase noise, the computational cost rises with the modulation order since more and more test phases are needed.

Because of the fourfold uncertainties of square QAM, the mentioned blind algorithms may result in cycle slip due to inaccurate phase estimation by a factor of π/2.

Nevertheless, differential encoding/decoding may be used to circumvent this issue, although at the cost of a little reduction in sensitivity. However, the higher computing cost is not always necessary to justify the gain [15].

v. Frequency Spreading (Fs) Equalization

In [8], author designed the novel equalization algorithm especially for multi carrier systems. The pictorial representation of this equalizer for FBMC OQAM is shown in Fig. 2.

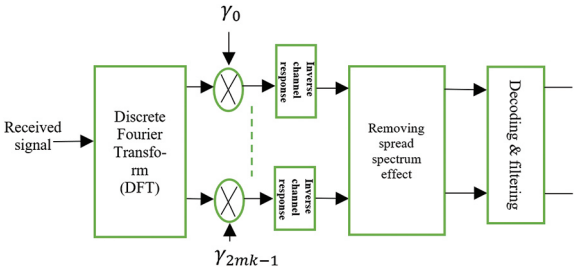

Fig. 2. Frequency Spreading equalizer

Input symbols propagated through the sub channel is spreader for number of sub carriers only if the corresponding samples of prototype filter (frequency domain) is non-zero. Spectral characteristics of the signal has been equalized after the received signal reach. Estimation of signal will not affect if the equalization done proper. Main advantage of this FS FBMC is no extra delay for computation.

vi. Overlap and Save Equalization

Researcher [9], proposed an overlap-save algorithm for equalization of single and multi-carrier systems. This algorithm provides the high efficiency in prediction of highest number of subcarriers from the finite impulse response (FIR). The procedure of the OS method is to prune the number of subcarriers for performing the convolution of FIR with each division of subcarriers in the frequency domain. In the initial stage, FFT is applied for each fragment, and it is convolved with frequency domain converted FIR signal. Once the convolution performed, the resultant will again convert back to time domain by IFFT and verified to $Kov/2$ overlapped symbols are included. Equalization is used to remove Inter Symbol Interference (ISI) from the received symbols, and Each symbol should be able to be recovered individually by the receiver [16]. Once equalized, the symbols are filtered by the FBMC prototype filter.

3. OPTICAL SYSTEM MODEL FOR THE FBMC-OQAM

Fig. 3 is a block diagram showing the FBMC OQAM Optical Communication system. The technology may be expanded to support dual polarization in addition to its single-polarization mode [17]. This method takes into account a subcarrier index of n, a QAM symbol time of T, and a subcarrier count of $2M$. The transmission of light across optical fibers may be affected by chromatic dispersion and AWGN channels [18].

FBMC transmitted signal with the rate of Fs=T/2M is generated as,

$$X(t) = \sum_{l=1}^{2N_s} \sum_{m=0}^{2M-1} q_{m,l} s_{m,l}(t) \tag{4}$$

where, $q_{m,l}$ is the OQAM modulated symbols, $s_{m,l}$ is the prototype filter response of FBMC synthesis filter and Ns is number of real multi carrier modulated symbols. Prototype filter is considered with the length of $L_p=2MO_k$. O_k is the overlapping factor of the filter with maximum energy and zero reconstruction error settings [19].

The chromatic dispersion frequency response of the channel propagation is defined as,

$$H(f) = e^{-j\frac{\pi D_c \lambda^2 F_l}{c} f^2} \tag{5}$$

where, F_l is Fiber length, D_c is Dispersion Coefficient, λ is laser wavelength, c is light speed and f is relative optical carrier frequency [20].

Distorted received signal after channel by impact of CD, Phase noise and additive noise is written as,

$$y(t) = \left(\int X(t) H(f) e^{j2\pi f t T_s} \, df + N(t) \right) e^{j\delta(t)} \tag{6}$$

Additive noise is representation of optical amplifier noise, thermal noise and short noise. Phase noise $\delta(t)$ is modelled as with linewidth of $\Delta\vartheta$ is,

$$\delta(t) = \delta(t-1) + \xi(t) \tag{7}$$

where, $\xi(t)$ is real Gaussian random value with zero mean and variance of $\sigma_\xi^2 = (\pi \Delta\vartheta T)/M$. The nonlinear phase noise shift effect is given as,

$$\delta(t) = \gamma L_{NF} \sum_{i=1}^{N_{span}} | X(t) + \sum_{j}^{O_k} N_A^j(t) |^2 \tag{8}$$

where, γ is the nonlinear coefficient and L_{NF} is nonlinear effective fiber length and is represented as,

$$L_{NF} = N_{span} \frac{(1 - e^{-\alpha L_{span}})}{\alpha} \tag{9}$$

α is fiber loss, L_{span} is fiber span length and N_{span} is number of 80km fiber spans. $N_A^j(t)$ is a noise of amplified spontaneous emission (ASE) and it is generated using AWGN with variance of σ^2 and zero mean. Hence the received signal after FBMC demodulation is given by,

$$Y_{m,l} = H_m \left(X_{m,l} + j\, r_{m,l} \right) e^{j\delta_l} + n_{m,l} \tag{10}$$

where, $r_{m,l}$ is the intrinsic interference of nearby symbols and $n_{m,l}$ is filtered additive noise. So the equalized symbol is formatted as,

$$\overline{X_{m,l}} = \sum_{l=0}^{N_{taps}} Y_{m,l} \, W_l \tag{11}$$

where, W_l is the equalization coefficients of the symbol using the proposed parallel analysis filter bank (AFB) equalization combined with Modified Blind Phase Search (MBPS) algorithm which detailed in section IV.

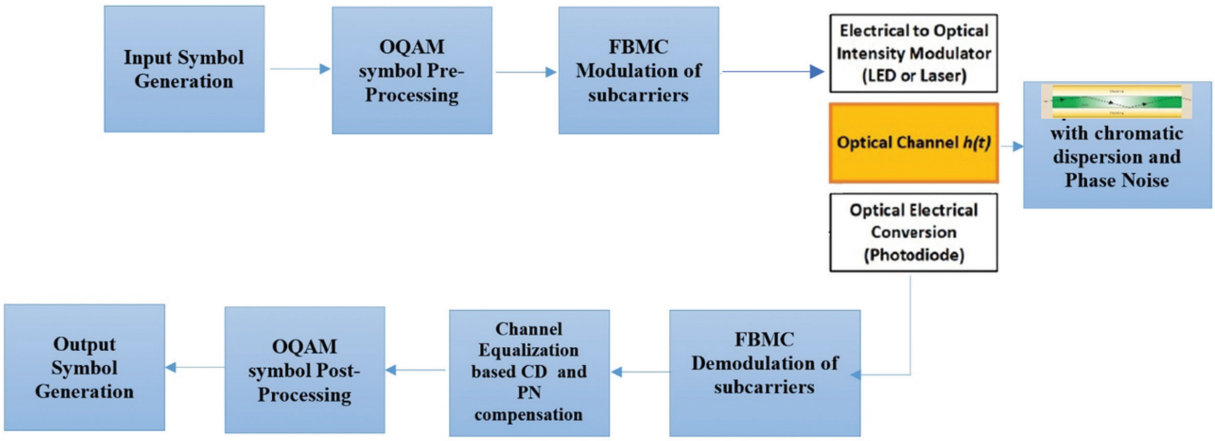

Fig. 3. Block Diagram of FBMC-OQAM Optical System

4. M-BPS WITH PARALLEL AFB FOR PHASE NOISE AND CHROMATIC DIFFUSION

Following the time-domain by using inverse fast Fourier transform process of frame synchronization, the received signal is sent on to the AFB block, where it will undergo frequency-domain processing. Similar to the approach used in [23, 24], a finite impulse response (FIR) filter is applied independently to each subcarrier to achieve CD correction. The core concept of the filter design is based on the frequency sampling method, which is extensively discussed in [25]. By manipulating the equalizer's coefficients, one may have the equalizer's frequency response "pass through" certain locations in the targeted subchannel. It is possible to calculate the equalizer's frequency response at certain frequencies using the zero-forcing criteria.

The configuration of parameters is listed in Table I. To show the exact performance of CD and PN compensation via proposed equalizers, For Each equalization some configurations are included as mentioned in Table 1. MSE and BER of received signal is calculated and compared for each subcarrier which taken as in Table 2, then we show the result in section v.

Table 1. Equalizer Parameters Configuration

Equalizer Type	Parameters and Values	
Multi Tap Equalizer	N_{taps}	3
ISDF Equalizer	N_{iter}	5
Parallel Equalization	K	3

Table 2. Constants Used in Simulations Configuration

Parameter	Value
Optical Fiber Length	1000 km
Dispersion Coefficient	17 ps/nm/km
Phase Noise Linewidth	200 KHz
Nonlinear coefficient	1.317 (1/W.km)
Fiber Type	SSMF
Core Effective Area	80μm²
Nonlinear Refractive Index	2.6×10^{-20} m²/W
Carrier Wavelength	1550 nm
Reference Bandwidth	12.5 GHz
Local Oscillator	Laser Source
Number of Subcarriers	128
FBMC overlapping factor	4
Modulation Order	16

The research suggests several different approaches to PN tracking [26-31]. Blind feedforward PN compensation gets our attention since it does not need the employment of pilots, which degrade spectral efficiency. The modified-blind phase search (M-BPS) technique has been found to give greater performance than the others [32], particularly when the number of subcarriers is considerable, despite its significant computing effort. The CD compensation block is by far the most difficult DSP step, therefore even while the complexity of the M-BPS increases with the order of the modulation, it has little impact on the complexity of the whole system [21]. As a result, we conduct this study with the M-BPS technique. You can read more about this method in [22]. Keep in mind that the little lingering CFO is also accounted for by the phase noise tracking.

A. Correction for Phase Noise using M-BPS

In order to fix the PN in the frequency domain, M-BPS is suggested [37]. The analysis filter bank (AFB) output data for all subcarriers are utilized to estimate the PN at each symbol time. The suggested methodology is so distinct from per-subcarrier PN compensation techniques. Using an analytical derivation, we demonstrate the algorithm's maximum likelihood (ML) optimality [38]. By just taking into account the distance in the real plane, M-BPS simplifies the computation of distance in the complex plane in comparison to other M-BPS algorithms. This drastically reduces the need for multiplication, which frees up more processing power for other tasks.

For the described system model in section III, a simple estimator for the absence of phase noise is made with removing the imaginary part to completely elimi-

nate the interference and considering only the real part of the equalized signal $\overline{X_{m,l}}$ as in (11).

When the phase noise presence the reconstruction of transmitted signal from the parallel AFB based equalized signal as,

$$\widehat{X_l} = \overline{X_l} \otimes \overline{\delta_l} + \overline{n_l} \tag{12}$$

where, $\widehat{X_l}$ is phase noise compensated signal after the MBPS algorithm and it is represented as,

$$\widehat{X_l} = \left[\widehat{X_{1,l}^R} \ \widehat{X_{1,l}^I} \ \widehat{X_{2,l}^R} \ \widehat{X_{2,l}^I} \ \ldots\ldots\ldots\ldots \widehat{X_{M,l}^R} \ \widehat{X_{M,l}^I} \right]^T \tag{13}$$

where $\widehat{X_{m,l}^R}$ and $\widehat{X_{m,l}^I}$ is real and imaginary part of phase noise compensated signal of m-th subcarrier and l-th modulated carrier. The phase noise signal $\overline{\delta_l}$ represented as,

$$\overline{\delta_l} = (\cos\delta_l \ \sin\delta_l)^T \tag{14}$$

$\bar{n}_l$ is denotes the equalized noise elements included with AWGN noise and interferences which represented by,

$$\overline{n_l} = \left[\overline{n_{1,l}^R} \ \overline{n_{1,l}^I} \ \overline{n_{2,l}^R} \ \overline{n_{2,l}^I} \ \ldots\ldots\ldots\ldots \overline{n_{M,l}^R} \ \overline{n_{M,l}^I} \right]^T \tag{15}$$

were,

$$\overline{n_{m,l}^R} = -r_{m,l}\sin\delta_l + n_{m,l}^R \tag{16}$$

$$\overline{n_{m,l}^I} = r_{m,l}\cos\delta_l + n_{m,l}^I \tag{17}$$

Where $\overline{n_{m,l}^R}$ and $\overline{n_{m,l}^I}$ is a real and imaginary elements of equalizers noise, Hence, we suggest testing all possible values of the phase, δ_K, on a predefined grid, and then choosing the value that minimizes the sum of distances between the projections on the real axis of the received samples after phase compensation testing and their hard decision counterparts [39]. The estimate and correction of phase noise is shown in Fig. 4.

The hard choice is done by picking the closest one between the projected values of the received sample and the optimal points of the pulse-amplitude modulation (PAM). The phase rotation used for a 4OQAM constellation is shown in Fig. 5. It is possible to express the expected phase rotation as,

$$\widehat{\delta_K} = \min_{\delta_K} \sum_{i=1}^{M} R[\overline{X_{\iota,l,K}}\ ] - H_d\left(R\left[\overline{X_{\iota,l,K}}\ \right]\right) \tag{18}$$

where, $R[.]$ denotes the real part of the signal and $H_d(.)$ represents the hard decision of phase search points. $\overline{X_{\iota,l,K}}$ is the rotated version of $\overline{X_{\iota,l}}$ given by,

$$\overline{X_{\iota,l,K}} = \overline{X_{\iota,l}}\, e^{-j\delta_K} \tag{19}$$

The phase search grid is defined as,

$$\delta_K = \frac{b}{B}\pi - \frac{\pi}{2} \tag{20}$$

Where B is the total number of phase tests and $b = 1, 2, B$. In order to lessen the effect of the additive noise, we average the cost function over M subcarriers. The switch then chooses the appropriate phase rotation to reduce the effect of phase noise by sending the samples' rotated versions in response to each phase test.

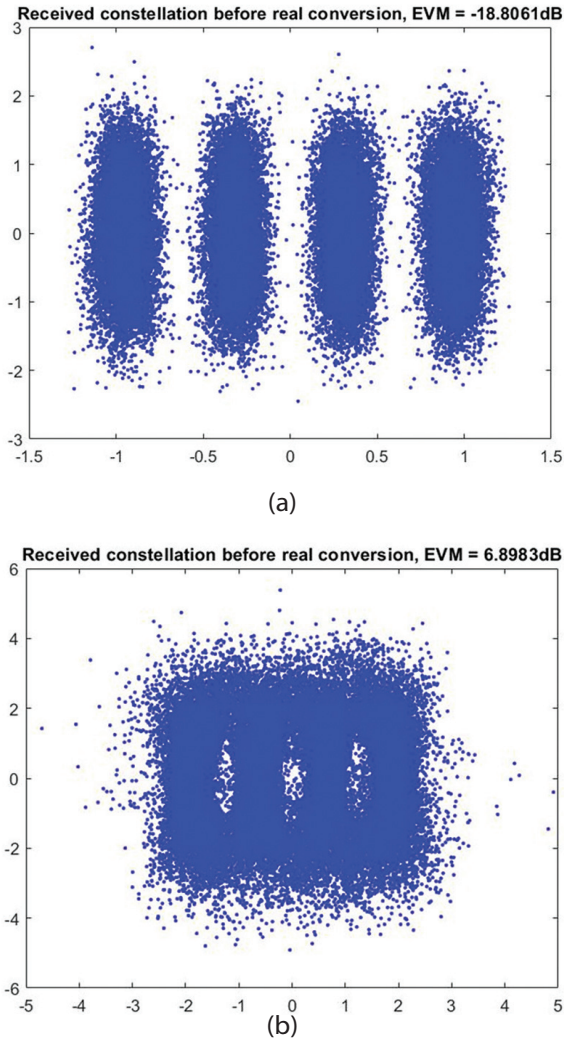

Fig. 4. modified blind phase search (M-BPS) (**a**) before and (**b**) after phase noise compensation

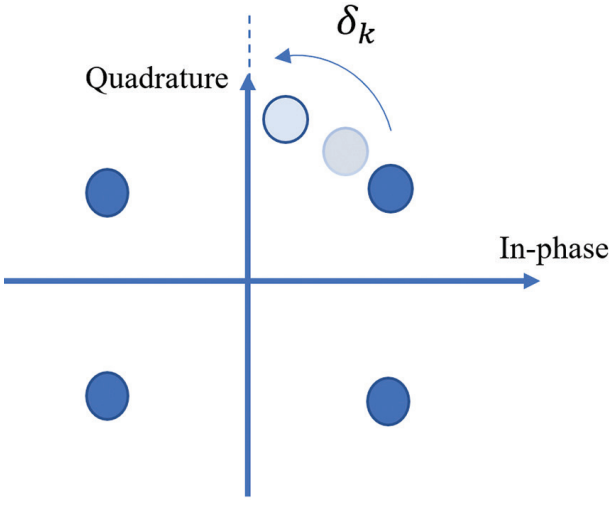

Fig. 5. Rotating the 4-OQAM constellation to measure the phase noise.

B. Features of M-BPS Estimation:

1. MBPS has a low computing cost and produces accurate phase noise estimations. In real-time systems [42], and this is important.

2. Due to its greater capture range, the MBPS approach can estimate phase noise even when the initial phase is far off [43]. This makes it resistant to severe channel faults such phase deviations or uncertain starting phases.

3. M-BPS estimator phase noise is accurate compering with other estimators such as maximum likelihood (ML), and Adaptive Maximum Likelihood (AML). M-BPS using iterative search. Through careful repetitions, the phase estimate approaches the true phase value. Phase noise may degrade FBMC performance, but this accuracy can compensate. As shown in Fig. 6.

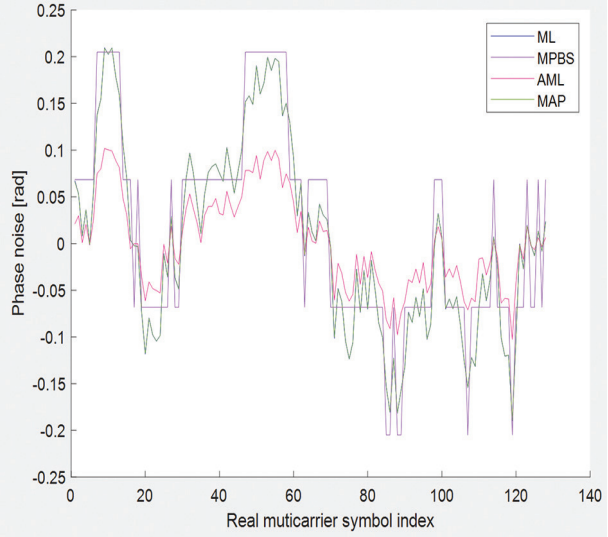

Fig. 6. Trackers By ML~MAP, AML, and M-BPS Estimators

4. The MBPS estimate is unaffected by fiber dispersion, temperature, or other channel variables. Due to its high channel flexibility, it can adjust for phase noise in many operational scenarios [44].

5. Modulation Format Independence MBPS works with several FBMC system configurations. It can be utilized in many optical fibers based FBMC topologies since it can compensate for phase noise in many system designs and handle many carrier frequencies.

C. Chromatic Dispersion Compensation Techniques

i. Single Tap Equalization

Low Complex single tap equalization is designed by [33], in which pre-equalization and equalization matrices are constructed. In general, multi-carrier systems split the bandwidth to number of narrow bands. Subcarrier counts in depends on the channel delay spread of FBMC OQAM. With the assumption of flat channel and slow varying phase noise single tap equalization is performed for the level of subcarrier [34]. Equalizer frequency response (FR) is calculated for the number of frequency points with the application of FIR filter and ZF reconstruction as shown in Fig. 7.

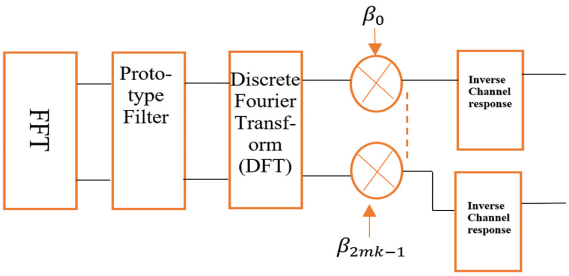

Fig. 7. Single Tap Equalization

Equalizer coefficient of one tap is given as,

$$\bar{z} = \frac{X_{m,n}}{H_m} e^{-j\beta_{m,n}} \tag{21}$$

where, $\beta_{m,n}$ is phase shift in prototype filter given by,

$$\beta_{m,n} = \frac{\pi}{2}(m+n) \tag{22}$$

$X_{m,n}$ is transmitted symbol of mth subcarrier and nth non equalized symbol, H_m is channel frequency response.

ii. The Equalization of multiple taps

The multi-tap equalization strategy models the secondary channel equalizers using a frequency sampling technique informed by channel information in the frequency space. The equalizer's coefficients are optimized such that the desired frequency filter response is attained. The transfer function of the filter is optimized to attain these predetermined values along the sub-channel frequency data. MMSE equalizer is one of the multi tap method which deals with the time domain coefficients which induce the successive interference cancellation (SIC) in throughput the system. For FBMC OQAM system frequency sampling based multi tap equalization is introduced by [35] as shown in Fig. 8. Equalizer coefficient is obtained for specific frequency points only by using channel impulse response (CIR) and is derived as,

$$\bar{z} = \left(\sum_{L=1}^{N_{taps}} W_{m,L} X_{m,n} \right) e^{-j\beta_{m,n}} \tag{23}$$

where, $W_{m,L}$ is weight of N_{taps} equalizer coefficients and it is derived for Zero Forcing (ZF) and Minimum Mean Square Error (MMSE) function in frequency sampling methodologies.

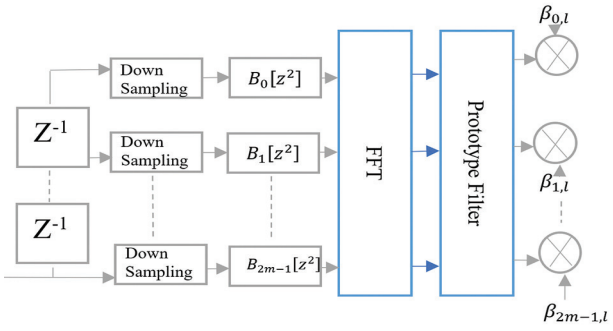

Fig. 8. Multi Tap Equalization

For ZF based equalization, W is described as,

$$W_Z = D_w^{-1} E_{zf} \tag{24}$$

where, E_{zf} is equalizer matrix for zeroforcing and is given by,

$$E_{zf} = (R_m^H R_m)^{-1} R_m^H \tag{25}$$

where, R_m is the frequency response matrix of N_t transmit antenna and Nr receive antenna at specific target points ϕ derived from Fourier transform of channel impulse response G_m and normalized impulse response G^n_m.

$$R_{m(N_t,N_r)} = \frac{\mathbb{F}(G_m)_\phi}{\mathbb{F}(G_m^n)_\phi} \tag{26}$$

Frequency target points of ϕ is calculated from the number of taps N_{taps} as,

$$\phi = \frac{2\pi}{N_{taps}+1}[-P, -P+1, \ldots\ldots, P] \tag{27}$$

Were,

$$P = \frac{(N_{taps}-1)}{2} \tag{28}$$

And Dw is equalizer weigh matrix calculated as,

$$D_{w(N_t,N_r)} = e^{jP\phi_{(N_t,N_r)}} \tag{29}$$

iii. Equalization using Parallel Analysis Filter Banks (AFBs)

A parallel multi tap equalizer is proposed by [36] to reduce the complexity of conventional multi tap equalization of FBMC OQAM. The graphical representation of this equalizer is depicted in Fig. 9. In this parallel AFBs equalization number of parallel receiver stage is structured in combiner part and all symbols are gathered based on per-subcarrier.

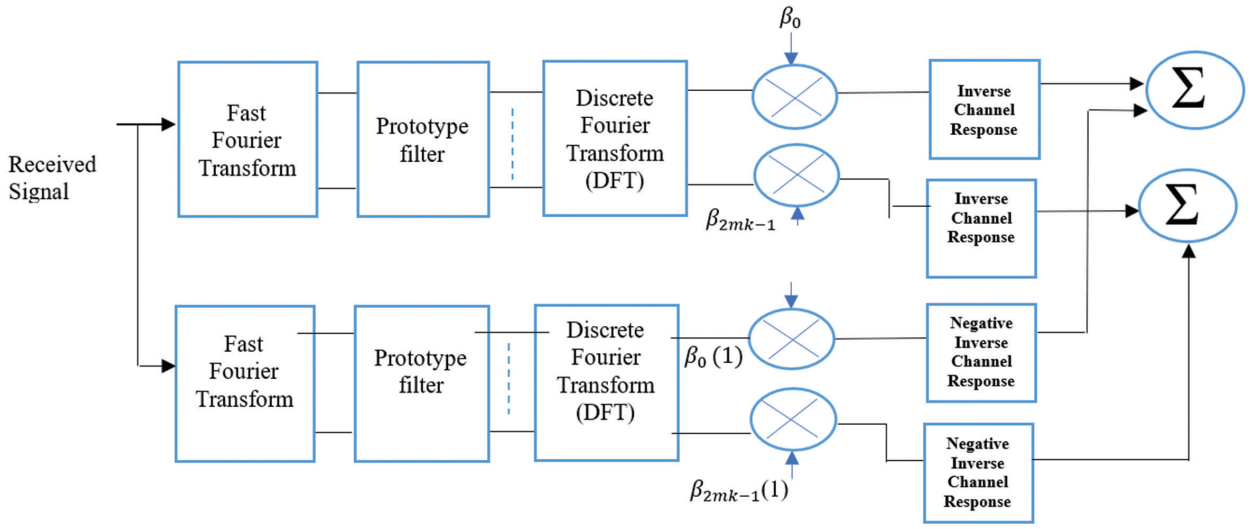

Fig. 9. Parallel AFB equalizer

For each K stages of equalization AFBs functions individualistically in parallel and principally filters the source signal by a polyphase network (PPN). This filter signal is derived from the received AFBs prototype pulse signal derivatives. Finally, the results from each stage are merged up to subcarrier level after performing the FFT. The equalization matrix is given by,

$$W_P = \sum_{k=0}^{K-1} \frac{J^k (H_m^{-1})^k}{(2M)^k} \tag{30}$$

5. RESULTS AND ANALYSIS

To prove the efficiency of multiple equalization for the purpose of CD and phase noise compensation in FBMC OQAM optical communication, in this section we perform the validation in terms of MSE, BER and Q-factor parameter. In this we are considering modulation of 16-OQAM. we are including the effects of phase noise (PN) and additive noise.

Using an optical amplifier with a noise figure anywhere from 0 to 30, Fig. 10 shows the bit error rate (BER) as a function of OSNR across a resolution bandwidth of 0.1 nm. As the OSNR increased BER getting reduced to $10^{-3.8}$ for our proposed parallel AFB with MBPS and for the same OSNR in ISDF-3-Tap reaches the $10^{-2.8}$. The Q-factor is computed from the bit error rate (BER) as [41].

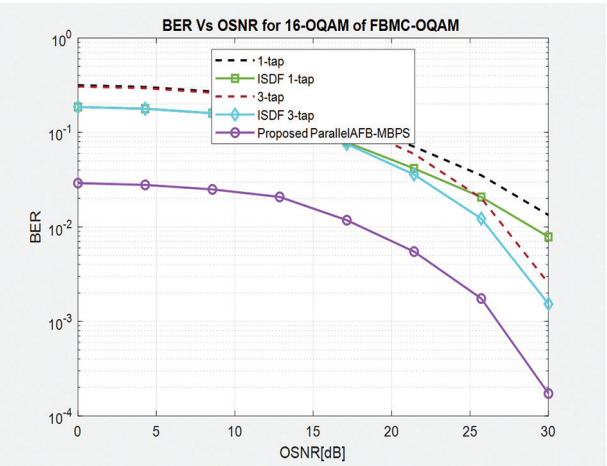

Fig. 10. BER Vs OSNR for 16-OQAM

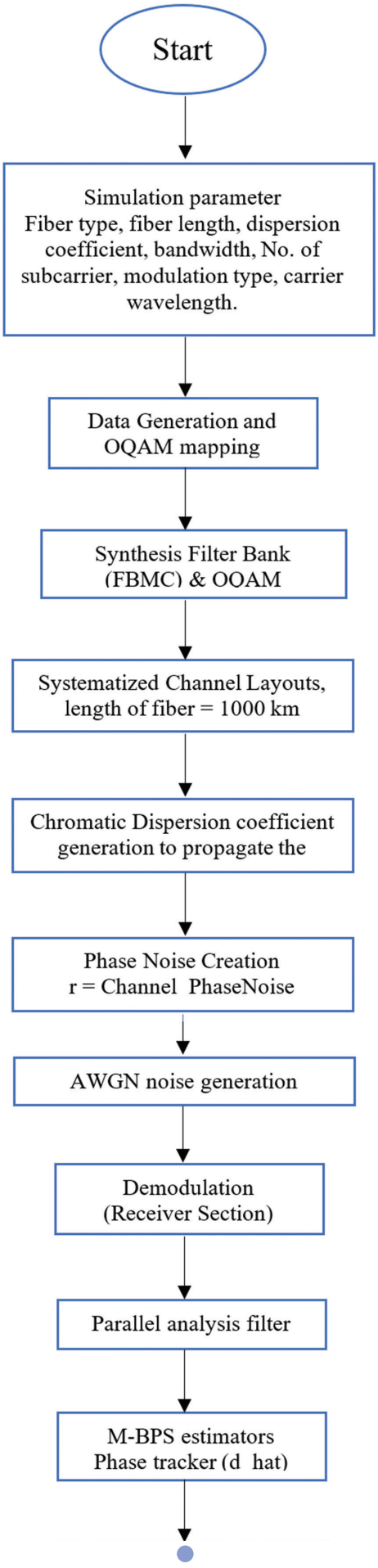

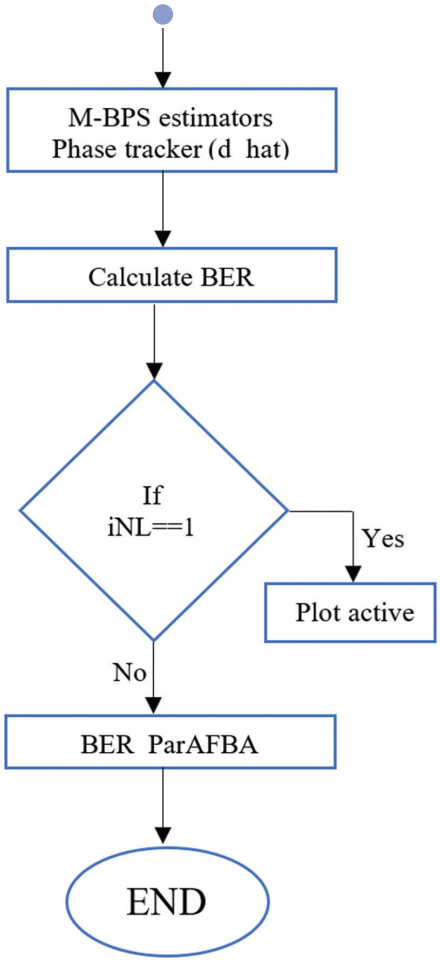

Fig. 11. flow chart of simulation FBMC/OQAM

$$Q_f(dB) = 20\log_{10}[\sqrt{2}\, erfc^{-1}(2 * BER)\,] \quad (31)$$

Q-factor is plotted versus OSNR with two separate Figs. of 11 and 12. Fig 12. shows the performance of Q-factor of different equalizers with fixed fiber length of 320 km.

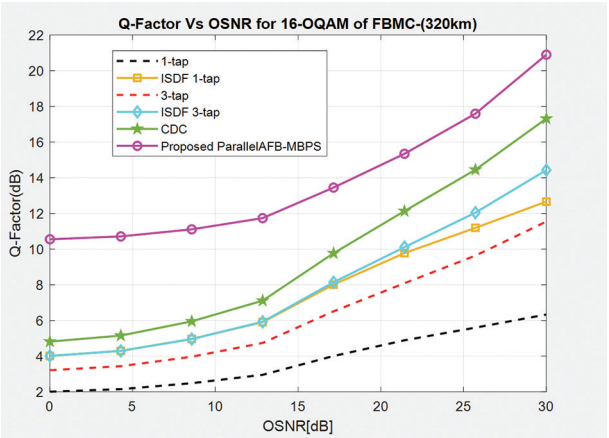

Fig. 12. Q-factor Vs OSNR for different Equalizer

Impact of different fiber length in Q-factor is reconnoitered for different equalizers and with consideration of OSNR metric with 0.1 nm resolution bandwidth as shown in Fig. 13, Fig. 14 and Fig. 15 respectively for

1-Tap ISDF, 3-Tap ISDF and Proposed Parallel AFB with MBPS equalizers.

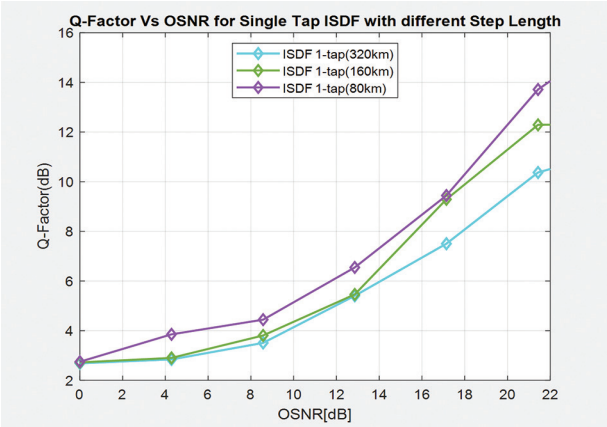

Fig.13. Q-factor Vs OSNR for different fiber length of ISDF-1-Tap equalizer

Fiber Length is configured with 320 km,160 km and 80 km for the implemented three equalizers of 1-Tap with ISDF, 3-Tap with ISDF and proposed Parallel AFB with MBPS. When the fiber length decreases the Q-factor getting increase as the information loss due to nonlinear effects are balances in short distance.

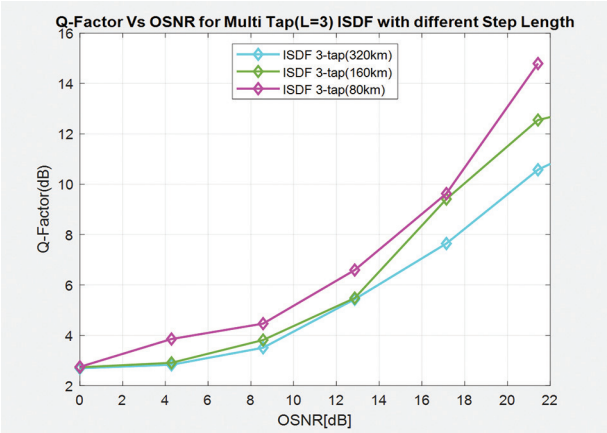

Fig. 14. Q-factor Vs OSNR for different fiber length of ISDF-3-Tap equalizer

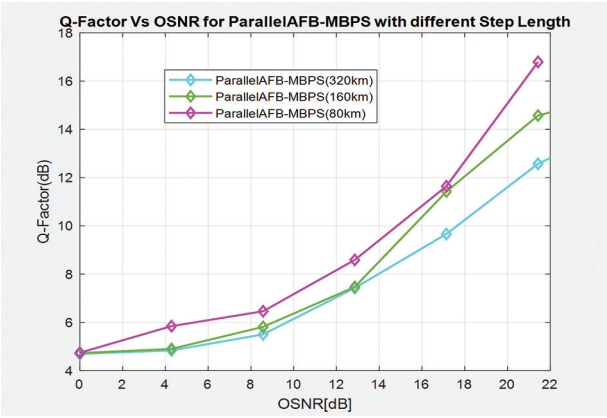

Fig. 15. Q-factor Vs OSNR for different fiber length of Parallel AFB with MBPS equalizer

BER Fig. 16 shows the results for varying fiber lengths and equalization settings. Fig. 16 depicts how the transmission distance of the fiber affects the BER performance of 16-QAM FBMC/OQAM. The anticipated fiber length is between 100 and 960 kilometers, with an 100-kilometer span. There were 24.19 dB, 21.18 dB, 19.42 dB, 18.17 dB, 17.2 dB, 16.41 dB, 15.74 dB, 15.16 dB, 14.19 dB, 13.78 dB, and 13.4 dB in received OSNR (0.1 nm resolution bandwidth) at various times. The findings are based on using a step length equal to the span length (80 km/step) or the entire fiber length (L/step) for equalization, and an input power of -10 dBm and an optical amplifier with a noise figure of 4 dB. Proposed parallel AFB with MBPS illustrated the improvement over other equalizers of ISDF and conventional multi tap equalizers for the entire fiber distance of low range to high range.

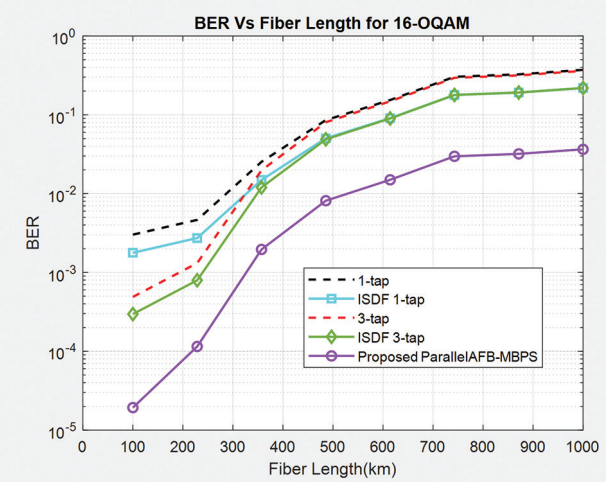

Fig.16. BER Vs Fiber Distance for different equalizer

The effect of carrier frequency offset lead to degradation the performance of the entire system which include interference between subcarriers, and intercarrier interference (ICI), and hence, lead to increase the BER.

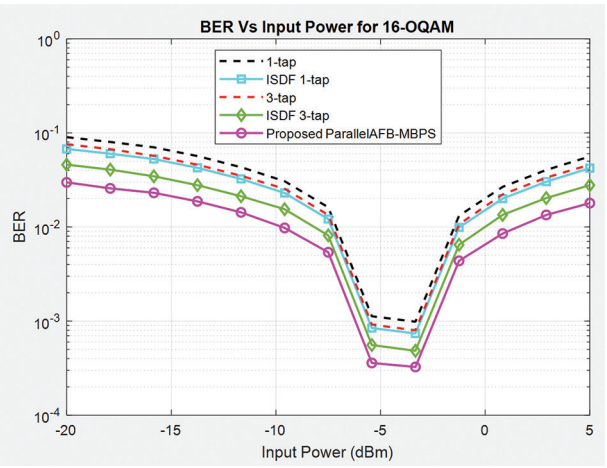

Fig. 17. BER Vs Input Power for different equalizer

Considering the SPM's interaction with ASE noise, as shown in Fig. 18, allows for an assessment of the FBMC/OQAM system's performance.

The bit error rate (BER) is shown vs signal strength. An optical amplifier with a noise figure of 4 dB is utilized to make up for the fiber loss in a 320-kilometer-long SSMF cable's transmission.

Figs. 18, 19, and 20 demonstrate that the BER performance of the ISDF-1-Tap equalization, ISDF-3-Tap equalizer, and the Parallel AFB with MBPS equalizer all increase with increasing input power when the system is running in the linear zone where the input power is less than 0 dBm. On the other hand, when input power is increased, nonlinear phase (NLP) noise degrades equalizer performance, leading to a lower bit error rate (BER). As a result, when nonlinear impairment is predominating, increasing the input power has a negative effect on the performance of the FBMC/OQAM system. Because of cumulative distortion from CD and NLP noise effects and the absence of a nonlinear compensator (NLC), a 1-tap equalizer cannot succeed. As compared to an ISDF-1-tap equalizer, the Parallel AFB with MBPS equalizer shows better results with optimal power at approximately -4 dBm.

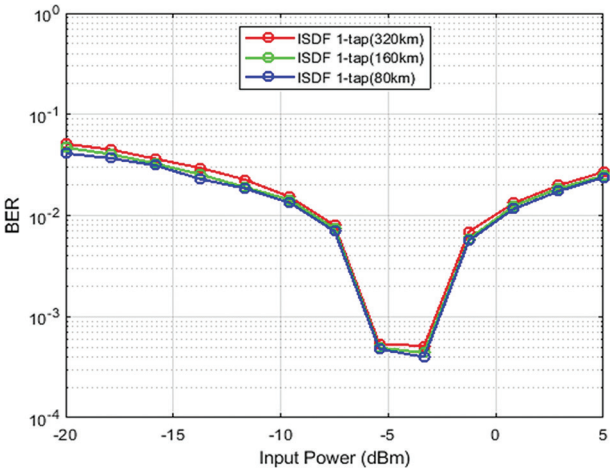

Fig. 18. BER Vs Input Power for ISDF-1-Tap equalizer

The ISDF and Parallel AFB equalizer with 80km/step length performs similarly to the case with 160km/step length at low input power.

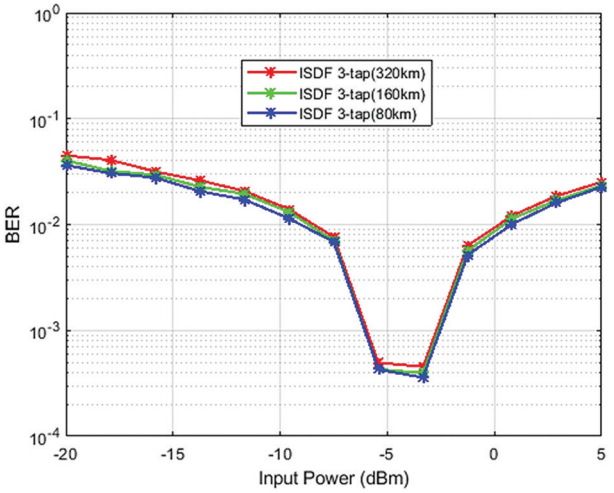

Fig. 19. BER Vs Input Power for ISDF-3-Tap equalizer

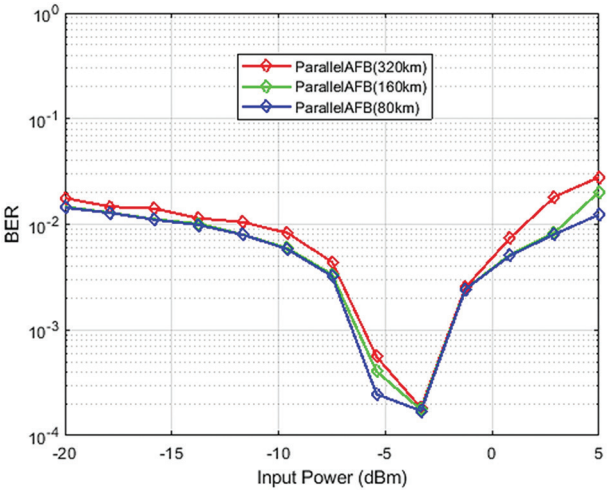

Fig. 20. BER Vs Input Power for Parallel AFB-MBPS equalizer

In summary, CD and nonlinear interference can be effectively removed by ISDF-1Tap (80 km/step) and parallel AFB with MBPS (80 km/step) equalizers. To enhance performance, though, they need to use a shorter step length.

When the transmitted power is huge, compensating just for the linear degradation is not enough. The fiber nonlinearity also plays a considerable role. When the fiber transmission distance is long, a system with a lot of power is required. The suggested equalizer is used to jointly adjust for the CD and phase noise (PN), and the results are compared to those obtained using the standard and benchmark equalizers. Filtering the CD-equalized signal using PN may help reduce the effects of fiber's nonlinear degradation.

To get the most out of your FBMC/OQAM setup, you'll need to optimize your NLC first. Several nonlinear (NL) scaling factors are shown in Fig. 21 to demonstrate the effect on the performance of the proposed parallel AFB with MBPS equalizers. The calculations use a noise figure of 4 dB per span and a transmission distance of 4 x 80 km.

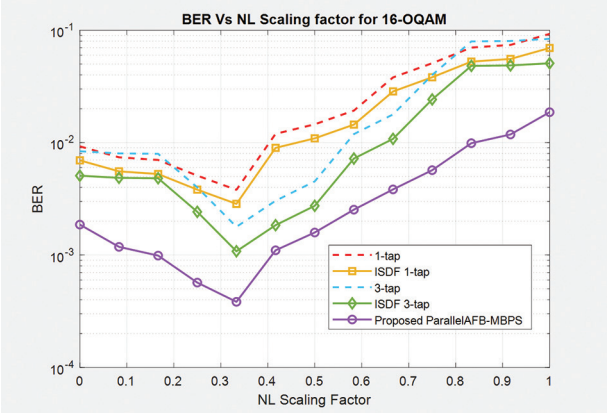

Fig. 21. BER Vs NL Scaling Factor for different equalizer

The nonlinearity area of the equalizers of ISDF-1-Tap, ISDF-3-Tap, and Parallel AFB with MBPS is shown in Fig. 22,

Fig. 23, and Fig. 24 to show the BER performance at a high input power of 2 dBm.

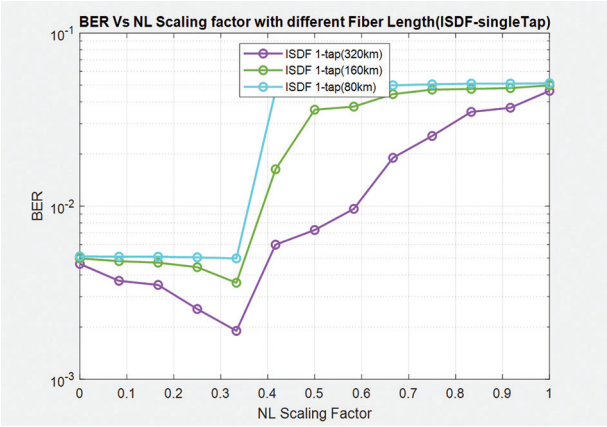

Fig. 22. BER Vs NL Scaling Factor for ISDF-1-Tap equalizer

As can be seen in Fig. 22, both the ISDF-1Tap (320km/step) and the ISDF-3Tap (320km/step) equalizers work optimally at a scale factor of 0.33.

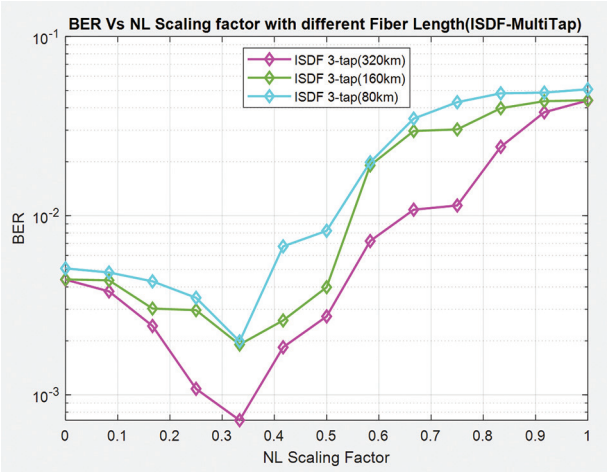

Fig. 23. BER Vs NL Scaling Factor for ISDF-3-Tap equalizer

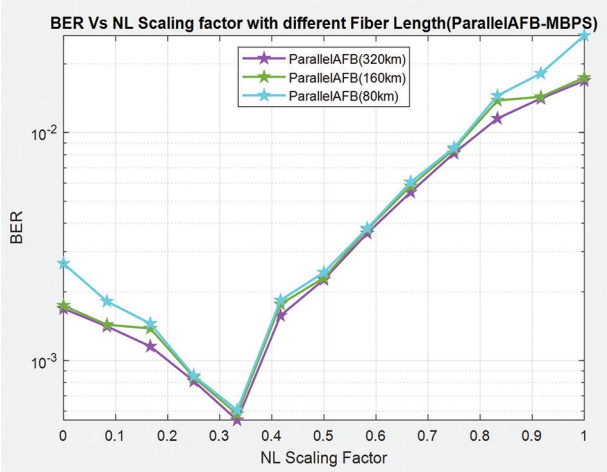

Fig. 24. BER Vs NL Scaling Factor for Parallel AFB-MBPS equalizer

Around 0.34 is the best scaling factor for the Parallel AFB-MBPS equalizer (80 km/step). For the Parallel AFB-MBPS equalizer to function at its best in terms of BER performance, as illustrated in Fig. 24, the NL scaling factor must be adjusted to its ideal value.

Fig. 25 displays MSE performance for a variety of equalizers and setups, all of which can be found in Table 1. At the bandwidth's edge, where the MSE is most extreme, the channel phase disparity is likewise the greatest. As the number of subcarriers increases, the system-wide chromatic dispersion is compensated for, leading to a decrease in MSE. We choose the often-used case of perfect CDC equalization for a single carrier [40] as our baseline for comparison. Fig. 25 shows that when the number of taps and the number of iterations in the ISDF both grow, the MSE's performance improves. However, these elements will add to the complexity of the system overall. Therefore, with its low complexity and little transmission latency, M-BPS based parallel AFB achieves the highest performance when compared to all these equalizers. ISDF-1-Tap technique provides MSE of difference of -14.1 dB, which is much better than one tap equalization. The MSE performance of ISDF with 3-Tap is -14.3 dB better than that of a 1-Tap equalizer. The findings of Parallel AFB with MBPS, however, show an improvement in MSE performance of -16.2 dB compared to that of 1-Tap.

By utilizing the different methodology that including AFB with MBPS, the experimental setup or simulation scenarios using the configuration parameter examine the performance metrics of each study to evaluate the effectiveness of the compensation technique to enhance MSE, BER, Power input, Q-factor and OSNR. Table (below) showing the difference finding studies.

Table 1. Comparison results between different studies

Parameters	Khaled A. Alaghbari 2020 [1]	Our Proposed Method
Mean square error	-13 dB	-16.2 dB
BER Vs. NL scaling factor for various equalizers (80,160,320) km	$10^{-1.5}$	$10^{-3.5}$
BER Vs. input power (80,160,320) km	~ 10^{-3} for various equalizers	$10^{-3.95}$
BER Vs. fiber length for 100 km	$10^{-3.7}$	$10^{-4.8}$
Q-factor Vs. OSNR for 0dB	~ 4 dB for different equalization	10.2 dB
Q-factor Vs. OSNR for 15 dB	~ 5.8 dB	12.2 dB

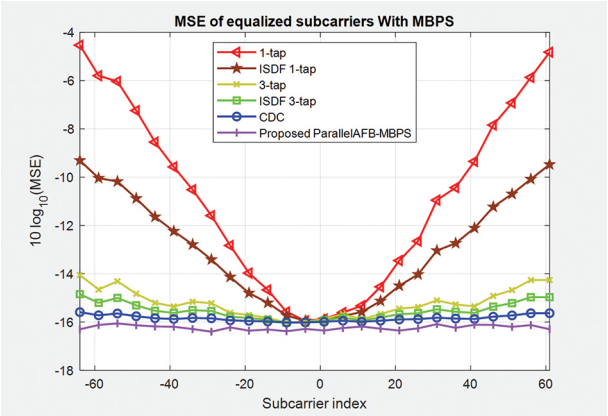

Fig. 25. MSE Vs Subcarrier Index

The 960 km ISDF-1Tap (L/step), ISDF-3Tap equalizers and parallel AFB-MBPS output are shown in Fig. 25, Fig. 26, and Fig. 27 respectively . High inter-symbol interference from CD, inherent interference, and optical channel noise distorts the constellation diagram at 960 km.

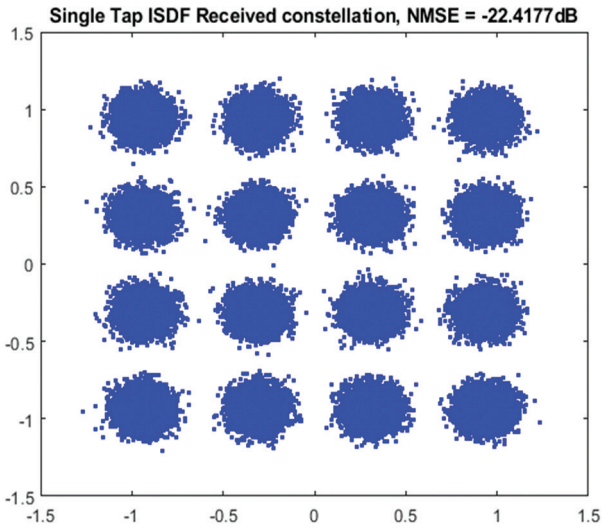

Fig. 25. 16-OQAM constellation of ISDF-1-Tap

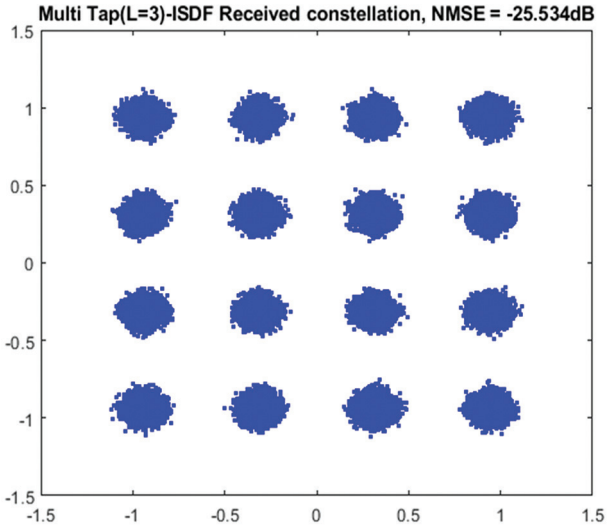

Fig. 26. 16-OQAM constellation of ISDF-3-Tap

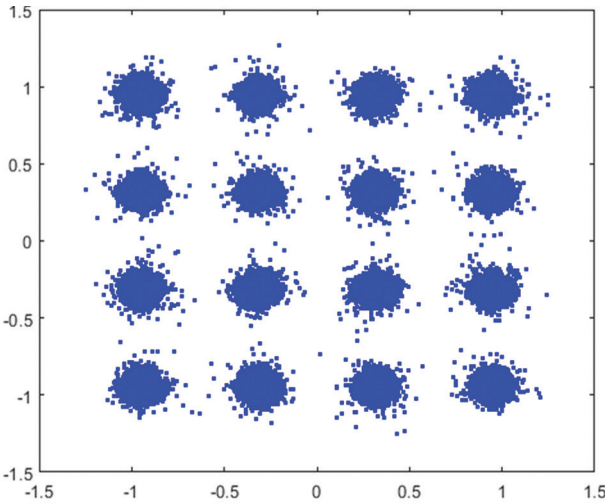

Fig. 27. 16-OQAM constellation of Parallel AFB-MBPS equalizer

6. CONCLUSION

Chromatic dispersion and phase noise in optical fiber communication with FBMC-OQAM protocol is compensated using parallel AFB with MBPS equalization method in this implementation. For comparison of proposed with previous equalizers of ISDF with single tap and multi tap is considered. These numerous equalizers are initially used in wireless transmission. In this work we are utilizing the concept of these equalizers in optical fiber FBMC OQAM. By increasing the number of subcarriers in the system will lead to phase noise. So here we achieve the best performance of both PN compensation and CD compensation in frequency and time domain with moderate subcarriers. Increasing the fiber length will affect the phase noise and degrade the BER performance of the system. After 700 km, the noise reaches the value where no data detection and BER approximately reaches the 0.5 value. The scaling factor affects the BER performance. The best scaling factor is obtained at 0.34 for the Parallel AFB-MBPS equalizer (80km/step).

In this we analyzed the complexity and performance for all compensation methods. Low complexity is achieved in proposed parallel AFB with modified blind phase search without any additional delay.

7. REFERENCES

[1] K. A. Alaghbari, H. S. Lim, T. A. Eltaif, "Compensation of chromatic dispersion and nonlinear phase noise using iterative soft decision feedback equalizer for coherent optical FBMC/OQAM systems", Journal of Lightwave Technology, Vol. 38, 2020, pp. 3839-3849.

[2] D. W. M. Guerra, T. Ab, "Efficient multitap equalization for FBMC-OQAM systems", Transactions on

Emerging Telecommunications Technologies, Vol. 30, No. 12, 2019, p. e3775.

[3] R. J. Essiambre, G. Kramer, P. J. Winzer, G. J. Foschini, B. Goebel, "Capacity limits of optical fiber networks", Journal of Lightwave Technology, Vol. 28, No. 4, 2010, pp. 662-701.

[4] F. Rottenberg, X. Mestre, F. Horlin, J. Louveaux, "Single-Tap Precoders and Decoders for Multi-User MIMO FBMC-OQAM under Strong Channel Frequency Selectivity", IEEE Transactions on Signal Processing, Vol. 65, No. 3, 2016, pp. 587-600.

[5] F. Rottenberg, T.-H. Nguyen, S.-P. Gorza, F. Horlin, J. Louveaux, "Advanced Chromatic Dispersion Compensation in Optical Fiber FBMC-OQAM Systems", IEEE Photonics Journal, Vol. 9, No. 6, 2017.

[6] Y.-F. Huang, C.T. Tsai, C.-Y. Chi, D.-W. Huang, G.-R. Lin, "Filtered Multicarrier OFDM Encoding on Blue Laser Diode for 14.8-Gbps Seawater Transmission", Journal of Lightwave Technology, Vol. 36, 2018, pp. 1739-1745

[7] H. Jamal, D. W. Matolak, "Dual-Polarization FBMC for Improved Performance in Wireless Communication Systems", IEEE Transactions on Vehicular Technology, Vol. 68, No. 1, 2019.

[8] H. Wang, W. Du, X. Wang, G. Yu, L. Xu, "Channel Estimation Performance Analysis of FBMC/OQAM Systems with Bayesian Approach for 5G-Enabled IoT Applications", Wireless Communications and Mobile Computing, Vol. 2020, 2020.

[9] J. Fickers, A. Ghazisaeidi, M. Salsi, G. Charlet, P. Emplit, F. Horlin, "Multicarrier Offset-QAM for Long-Haul Coherent Optical Communications", Journal of Lightwave Technology, Vol. 32, No. 24, 2014.

[10] Z. Li, "Experimental demonstration of 110-Gb/s unsynchronized band-multiplexed superchannel coherent optical OFDM/OQAM system", Optics Express, Vol. 21, No. 19, 2013, pp. 21924-21931.

[11] M. Bellanger, "FS-FBMC: an alternative scheme for filter bank based multicarrier transmission", Proceedings of the 5th International Symposium on Communications, Control and Signal Processing, Rome, Italy, 2-4 May 2012.

[12] T.-H. Nguyen, J. Louveaux, S. P. Gorza, F. Horlin, "Simple feedforward carrier phase estimation for optical FBMC/OQAM systems", IEEE Photonics Technology Letters, Vol. 28, No. 24, 2016, pp. 2823-2826.

[13] T.-H. Nguyen, F. Rottenberg, S. P. Gorza, J. Louveaux, F. Horlin, "Efficient chromatic dispersion compensation and carrier phase tracking for optical fiber FBMC/OQAM systems", Journal of Lightwave Technology, Vol. 35, No. 14, 2017, pp. 2909-2916.

[14] T.-H. Nguyen et al. "Experimental Demonstration of the Tradeoff Between Chromatic Dispersion and Phase Noise Compensation in Optical FBMC/OQAM Communication Systems", Journal of Lightwave Technology, Vol. 37, 2019, 4340-4348.

[15] S. Chimmalgi, A. Rode, L. Schmid, L. Schmalen, "Approximate Maximum a Posteriori Carrier Phase Estimator for Wiener Phase Noise Channels using Belief Propagation", arXiv:2307.03517, 2023.

[16] X. Mestre, M. Majoral, S. Pfletschinger "An Asymptotic Approach to Parallel Equalization of Filter Bank Based Multicarrier Signals", IEEE Transactions on Signal Processing, Vol. 61, No. 14, 2013.

[17] L. Zhang, P. Xiao, A. Zafar, A. Quddus, R. Tafazolli, "FBMC system: an insight into doubly dispersive channel impact", IEEE Transactions on Vehicular Technology, Vol. 66, No. 5, 2016, pp. 3942-3956.

[18] M. Ionescu, D. Lavery, A. Edwards, E. Sillekens, L. Galdino, D. Semrau, R. I. Killey, W. Pelouch, S. Barnes, P. Bayvel, "74.38 Tb/s transmission over 6300 km single mode fiber with hybrid EDFA/Raman amplifiers", Proceedings of the Optical Fiber Communication Conference, San Diego, CA, USA, 3-7 March 2019.

[19] P. J. Winzer, D. T. Neilson, A. R. Chraplyvy, "Fiber-optic transmission and networking: the previous 20 and the next 20 years", Optics Express, Vol. 26, No. 18, 2018, pp. 24190-24239.

[20] K. Zanette, J. C. Cartledge, M. O'Sullivan, "Correlation properties of the phase noise between pairs of lines in a quantum-dot optical frequency comb source", Proceedings of the Optical Fiber Communication Conference, Los Angeles, CA, USA, 19-23 March 2017.

[21] G. Vedala, M. Al-Qadi, M. O'Sullivan, J. Cartledge, R. Hui, "Phase noise characterization of a QD-based

diode laser frequency comb", Optics Express, Vol. 25, No. 14, 2017, pp. 15890-15904.

[22] C. Antonelli, O. Golani, M. Shtaif, A. Mecozzi, "Nonlinear interference noise in space-division multiplexed transmission through optical fibers", Optics Express, Vol. 25, No. 12, 2017, pp. 13055-13078.

[23] C. Li, Q. Yang, "Optical OFDM/OQAM for the future ber optics communications", Procedia Engineering, Vol. 140, 2016, pp. 99-106.

[24] M. Bi, L. Zhang, L. Liu, G. Yang, R. Zeng, S. Xiao, Z. Li, Y. Song, "Experimental demonstration of the OQAM-OFDM-based wavelength stacked passive optical networks", Optics Communications, Vol. 394, 2017, pp. 129-134.

[25] D. Petrovic, W. Rave, G. Fettweis, "Effects of phase noise on OFDM systems with and without PLL: Characterization and compensation", IEEE Transactions on Communications, Vol. 55, No. 8, 2007, pp. 1607-1616.

[26] F. Rottenberg, T.-H. Nguyen, S.-P. Gorza, F. Horlin, J. Louveaux, "ML and MAP phase noise estimators for optical fiber FBMC-OQAM systems", Proceedings of the IEEE International Conference on Communications, Paris, France, 21-25 May 2017, pp. 1-6.

[27] T. T. Nguyen, S. T. Le, R. Nissel, M. Wuilpart, L. Van Compernolle, P. Megret, "Pseudo-pilot coding-based phase noise estimation for coherent optical FBMC-OQAM transmissions", Journal of Lightwave Technology, Vol. 36, No. 14, 2018, pp. 2859-2867.

[28] B. You, L. Yang, F. Luo, S. Fu, S. Yang, B. Li, D. Liu, "Joint carrier frequency offset and phase noise estimation based on pseudo-pilot in CO-FBMC/OQAM system", IEEE Photonics Journal, Vol. 11, No. 1, 2019, pp. 1-11.

[29] X. Yan et al. "Low-complexity carrier phase estimation for M-ary quadrature amplitude modulation optical communication based on dichotomy", Optics Express, Vol. 28, No. 17, 2020, pp. 25263-25277.

[30] T.-H. Nguyen, C. Peucheret, "Kalman Filtering for Carrier Phase Recovery in Optical Offset-QAM Nyquist WDM systems", IEEE Photonics Technology Letters, Vol. 29, No. 12, 2017, pp. 1019-1022.

[31] J. Zhao, "Format-transparent phase estimation based on KL divergence in coherent optical systems", Optics Express, Vol. 28, No. 14, 2020, pp. 20016-20031.

[32] T. Sasai, A. Matsushita, M. Nakamura, S. Okamoto, F. Hamaoka, Y. Kisaka, "Laser phase noise tolerance of uniform and probabilistically shaped QAM signals for high spectral efficiency systems", IEEE/OSA Journal of Lightwave Technology, Vol. 38, No. 2, 2020, pp. 439-446.

[33] P. Zhang, H. Ren, M. Gao, J. Lu, Z. Le, Y. Qin, W. Hu, "Low-complexity blind carrier phase recovery for C-mQAM coherent systems", IEEE Photonics Journal, Vol. 11, No. 1, 2019, p. 7200214.

[34] Q. Xiang, Y. Yang, Q. Zhang, Y. Yao, "Low complexity, modulation transparent and joint polarization and phase tracking scheme based on the nonlinear principal component analysis", Optics Express, Vol. 27, No. 13, 2019, pp. 17968-17978.

[35] M. Nouri, M. G. Shayesteh, N. Farhangian, "Chromatic Dispersion and Nonlinear Phase Noise Compensation Based on KLMS Method", Optics Communications, Vol. 351, 2015, pp. 149-154.

[36] J. Louveaux "Equalization and Demodulation in the Receiver (Single Antenna)", PHYDYAS Technical Report, ICT-211887, 2008.

[37] T. Ihalainen, A. Ikhlef, J. Louveaux, M. Renfors "Channel Equalization for Multi-Antenna FBMC/OQAM Receivers", IEEE Transactions on Vehicular Technology, Vol. 60, No. 5, 2011, pp. 2070-2085.

[38] K. A. Alaghbari, H. S. Lim, T. Eltaif, N. Alsowaidi, "Chromatic Dispersion Compensation for Offset-QAM/FBMC Based Coherent WDM Using Digital Filter", Proceedings of the IEEE 7th International Conference on Photonics, Kuah, Malaysia, 9-11 April 2018, pp. 1-3.

[39] P. Duhamel, M. Vetterli, "Fast Fourier Transforms: A Tutorial Review and a State of the Art", Signal Processing Journal, Vol. 19, No. 4, 1990, pp. 259-299.

[40] A. Viholainen, M. Bellanger, M. Huchard, "Prototype Filter and Structure Optimization", PHYDYAS Technical Report, 2009.

[41] A. Zaidi, F. Athley, J. Medbo, U. Gustavsson, G. Durisi, X. Chen, "5G Physical Layer: Principles, Models and Technology Components", 1st Edition, Academic Press, 2018.

[42] Y. Shao et al. "Phase noise model for continuous-variable quantum key distribution using a local local oscillator", Physical Review A, Vol. 104, No. 3, 2021.

[43] B. You et al. "Joint carrier frequency offset and phase noise estimation based on pseudo-pilot in CO-FBMC/OQAM system", IEEE Photonics Journal, Vol. 11, No. 1, 2019, pp. 1-11.

[44] E. Börjesson, "Implementation of Blind Carrier Phase Recovery for Coherent Fiber-Optical Receivers", University of Gothenburg, Gothenburg, Sweden, 2018, Master thesis.